Mon. Not. R. Astron. Soc. **000**, 000–000 (0000) Printed 21 October 2015 (MN LATEX style file v2.2)

Galaxy Zoo: Evidence for rapid, recent quenching across a population of AGN host galaxies

R. J. Smethurst,[1] C. J. Lintott,[1] B. D. Simmons,[1] K. Schawinski,[2] S. P. Bamford,[3] C. N. Cardamone,[4] S. J. Kruk,[1] K. L. Masters,[5] C. M. Urry,[6] K. W. Willett,[7] O. I. Wong[8] ⋆

[1] *Oxford Astrophysics, Department of Physics, University of Oxford, Denys Wilkinson Building, Keble Road, Oxford, OX1 3RH, UK*
[2] *Institute for Astronomy, Department of Physics, ETH Zurich, Wolfgang-Pauli Strasse 27, CH-8093 Zürich, Switzerland*
[3] *School of Physics and Astronomy, The University of Nottingham, University Park, Nottingham, NG7 2RD, UK*
[4] *Math & Science Department, Wheelock College, 200 The Riverway, Boston, MA 02215, USA*
[5] *Institute of Cosmology and Gravitation, University of Portsmouth, Dennis Sciama Building, Barnaby Road, Portsmouth, PO1 3FX, UK*
[6] *Department of Physics and Yale Center for Astronomy and Astrophysics, Yale University, PO Box 208121, New Haven, CT 06520-8121, USA*
[7] *School of Physics and Astronomy, University of Minnesota, 116 Church St SE, Minneapolis, MN 55455, USA*
[8] *International Centre for Radio Astronomy Research, UWA, 35 Stirling Highway, Crawley, WA 6009, Australia*

21 October 2015

ABSTRACT

We present a population study of the star formation history of 1,244 Type 2 AGN host galaxies, compared to 123,243 inactive galaxies using a Bayesian method. We find evidence for the Type 2 AGN host galaxies having undergone a recent (within 2 Gyr) and rapid drop in their star formation rate. AGN feedback is therefore important at least for this population of galaxies. This result is not seen for the inactive galaxies whose star formation histories are dominated by the effects of downsizing at earlier epochs, a secondary effect for the AGN host galaxies. We show that histories of rapid quenching cannot account fully for the quenching of all the star formation in a galaxy's lifetime across the population of AGN host galaxies, and that histories of slower quenching, attributed to secular (non-violent) evolution, are also key in their evolution. This is in agreement with recent results showing both merger-driven and non-merger processes are contributing to the co-evolution of galaxies and supermassive black holes. The availability of gas in the reservoirs of a galaxy, and its ability to be replenished, appear to be the key drivers behind this co-evolution.

1 INTRODUCTION

The nature of the observed co-evolution of galaxies and their central supermassive black holes (Magorrian et al. 1998; Marconi & Hunt 2003; Haring & Rix 2004) and the effects of AGN feedback on galaxies are two of the most important open issues in galaxy evolution. AGN feedback was first suggested as a mechanism for regulating star formation in simulations (Silk & Rees 1998; Croton et al. 2006; Bower et al. 2006; Somerville et al. 2008) and some indirect evidence has been observed for both positive and negative feedback in various systems (see the comprehensive review from Fabian 2006).

The strongest observational evidence for AGN feedback in a population is that the largest fraction of AGN are found in the green valley (Cowie & Barger 2008; Hickox et al. 2009; Schawinski et al. 2010), suggesting some link between AGN activity and the process of quenching which moves a galaxy from the blue cloud to the red sequence. However, concrete statistical evidence for the effect of AGN feedback on the host galaxy population has so far been elusive.

Here we present a large observational population study of the quenching of Type 2 AGN the host galaxies identified by line diagnostics. We use a new Bayesian method (Smethurst et al. 2015) to effectively determine the most probable SFH of a galaxy, modelled with two parameters, time of quenching, t_q, and exponential rate, τ, given the observed near ultra-violet (NUV) and optical colours. This builds on the work of Martin et al. (2007) and Schawinski et al. (2014), however this study demonstrates a significant improvement over these previous studies through the use of a Bayesian-MCMC methodology. Through this we aim to determine the following: (i) Are galaxies currently hosting an AGN undergoing quenching? (ii) If so, when and at what rate does this quenching occur? (iii) Is this quenching occurring at different times and rates compared to a control sample of inactive galaxies?

The zero points of all magnitudes are in the AB sys-

⋆ This investigation has been made possible by the participation of over 350,000 users in the Galaxy Zoo project. Their contributions are acknowledged at `http://authors.galaxyzoo.org`

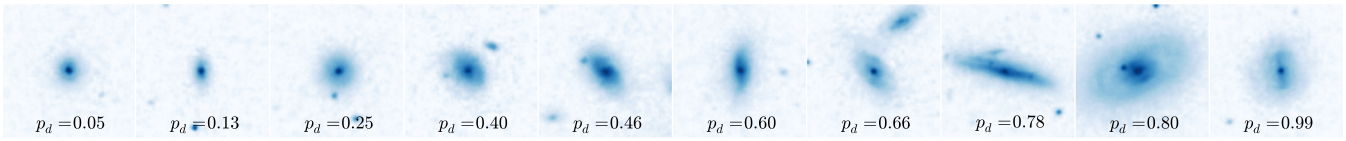

Figure 1. Randomly selected SDSS *gri* composite images from the sample of 1,244 Type 2 AGN in a redshift range $0.04 < z < 0.05$. The galaxies are ordered from least to most featured according to their debiased 'disc or featured' vote fraction, p_d (see Willett et al. 2013). The scale for each image is 0.099 arcsec/pixel.

tem and where necessary, we adopt the WMAP Seven-Year Cosmology (Jarosik et al. 2011) with $(\Omega_m,\ \Omega_\Lambda,\ h) = (0.26, 0.73, 0.71)$.

2 DATA & METHODS

In this investigation we use visual classifications of galaxy morphologies from the Galaxy Zoo 2[1] (GZ2) citizen science project (Willett et al. 2013), which obtains multiple independent classifications for each optical image. The full question tree for an image is shown in Figure 1 of Willett et al. The GZ2 project used 304,022 images from the Sloan Digital Sky Survey Data Release 7 (SDSS; York et al. 2000; Abazajian et al. 2009) all classified by *at least* 17 independent users, with a mean number of classifications of ~ 42.

Further to this, we required NUV photometry from the GALEX survey (Martin et al. 2005), within which $\sim 42\%$ of the GZ2 sample was observed, giving 126,316 galaxies total $(0.01 < z < 0.25)$. This will be referred to as the GZ2-GALEX sample. The completeness of this sample $(-22 < M_u < -15)$ is shown in Figure 2 of Smethurst et al. (2015).

Observed fluxes are corrected for galactic extinction (Oh et al. 2011) by applying the Cardelli et al. (1989) law. We also adopt k-corrections to $z = 0.0$ and obtain absolute magnitudes from the NYU-VAGC (Blanton et al. 2005; Padmanabhan et al. 2008; Blanton & Roweis 2007).

2.1 Bayesian SFH Determination

STARPY[2] is a PYTHON code which allows the user to derive the quenched star formation history (SFH) of a galaxy through a Bayesian Markov Chain Monte Carlo method (Foreman-Mackey et al. 2013)[3] with the input of the observed $u-r$ and $NUV-u$ colours, a redshift, and the use of the stellar population models of Bruzual & Charlot (2003). These models are implemented using solar metallicity (the effect of using a different metallicity was investigated in Smethurst et al. 2015) and a Chabrier IMF (Chabrier et al. 2003). The star formation history template is an exponential decline of the SFR and is described by two parameters $[t_q, \tau]$, where t_q is the time at which the onset of quenching begins [Gyr] and τ is the exponential rate at which quenching occurs [Gyr]. Under the simplifying assumption that all galaxies formed at $t = 0$ Gyr with an initial burst of star formation, the SFH can be described as:

$$SFR = \begin{cases} i_{sfr}(t_q) & \text{if } t < t_q \\ i_{sfr}(t_q) \times exp\left(\frac{-(t-t_q)}{\tau}\right) & \text{if } t > t_q \end{cases} \quad (1)$$

where i_{sfr} is an initial constant star formation rate dependent on t_q (Schawinski et al. 2014; Smethurst et al. 2015). A smaller τ value corresponds to a rapid quench, whereas a larger τ value corresponds to a slower quench. This SFH model has previously been shown as appropriate for describing quenching galaxies by Weiner et al. (2006); Martin et al. (2007); Noeske et al. (2007) and Schawinski et al. (2014).

The probabilistic fitting methods to this SFH for an observed galaxy are described in full detail in Section 3.2 of Smethurst et al. (2015) wherein the STARPY code was used to characterise the SFHs of the GZ2-GALEX sample. We assume a flat prior on all the model parameters and a double gaussian likelihood function for the $u-r$ and $NUV-u$ colours (Equation 2 in Smethurst et al. 2015). The output of STARPY is probabilistic in nature and provides the posterior probability distribution across the entirety of the two parameter space for an individual galaxy. To study the SFH across a given population of galaxies, these individual posterior probability distributions can be combined by summing each binned distribution. We also utilise the GZ debiased vote fractions to obtain separate summed posterior probability distributions for both smooth and disc galaxies; obtained by weighting by either the disc, p_d or smooth, p_s vote fraction of each galaxy when summing, as in Smethurst et al. (2015). This ensures that the entirety of the population is used, with galaxies with a higher p_d contributing more to the disc weighted than the smooth weighted posterior distribution. This negates the need for a threshold on the GZ vote fractions (e.g. $p_d > 0.8$), unlike in previous studies (Schawinski et al. 2014).

2.2 AGN Sample

We selected Type 2 AGN using a BPT diagram (Baldwin, Phillips & Terlevich 1981) using line and continuum strengths for [OIII], [NII], [SII] and [OII] obtained from the MPA-JHU catalogue (Kauffman et al. 2003a; Brinchmann et al. 2004) for galaxies in the GZ2-GALEX sample. We then required the S/N > 3 for each emission line as in Schawinski et al. (2010). Those galaxies which satisfied all of the inequalities defined in Kewley et al. (2001) and Kauffman et al. (2003b) were selected as Type 2 AGN, giving 1,299 host galaxies ($\sim 10\%$ of the GZ2-GALEX sample). Sarzi et al. (2010); Yan & Blanton (2012) and Singh et al. (2013) have all demonstrated that LINERs are not primarily powered by AGN, therefore for purity, we excluded these galaxies from the sample using the definition from Kewley et al. (2006) (55

[1] `http://zoo2.galaxyzoo.org/`
[2] Publicly available: `http://github.com/zooniverse/starpy`
[3] `http://dan.iel.fm/emcee/`

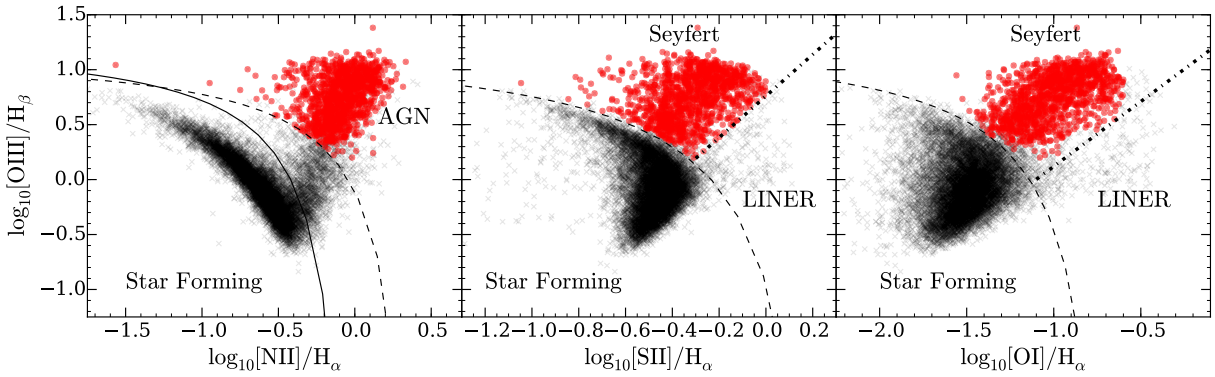

Figure 2. BPT diagrams for galaxies in the GZ2-GALEX sample (black crosses) with S/N > 3 for each emission line. Inequalities defined in: Kewley et al. (2001) to separate SF galaxies from AGN (dashed lines), Kauffman et al. (2003b) to separate SF from composite SF-AGN galaxies (solid line) and Kewley et al. (2006) to separate LINERS and Seyferts (dotted lines). Galaxies are included in the AGN-HOST sample (red circles) if they satisfy all the inequalities to be classified as Seyferts. LINERs are excluded for purity.

galaxies total) with no change to the results. These 1,244 galaxies will be referred to as the AGN-HOST sample.

Type 2 AGN were used in this analysis as opposed to Type 1 due to their photometric obscuration. Type 1 AGN contaminate their galaxy's photometric measurements which would need to be removed through aperture matching. Due to the requirement for NUV colours from GALEX, in order to be sensitive to any recent star formation, the aperture matching to SDSS becomes a non-trivial task.

Simmons et al. (2011) showed that the obscuration of a Type 2 AGN is more efficient in the NUV than in the optical. Residual NUV flux from the AGN can thus be neglected in comparison to that of the galaxy. However there is often some residual optical flux that can affect the measurements of the host galaxy's photometry. We can subtract this central optical AGN flux using the magnitudes provided by SDSS fit to a central point spread function (PSF), however the change in the colours of these galaxies after this correction is negligible, with $\Delta(u-r) \sim 0.09$. We therefore use the uncorrected colours to avoid unnecessary complexity and minimise the propagation of uncertainty from the colours through to the SFHs. Including these corrected colours does not change the results described below.

Image from SDSS for ten randomly selected galaxies from the AGN-HOST sample are shown in Figure 1 and Figure 2 shows the entire AGN-HOST sample and the matched GZ2-GALEX galaxies on a BPT diagram. For the AGN-HOST sample the mean $\log(L[OIII]$ [erg s^{-1}]$) \sim 41.3$ and median $\log(L[OIII]$ [erg s^{-1}]$) \sim 41.0$, with a range of $\log(L[OIII]$ [erg s^{-1}]) luminosities of $39.4 - 43.0$.

We constructed a sample of inactive galaxies by removing from the GZ2-GALEX sample all those galaxies above the Kauffman et al. (2003b) line separating star forming from active galaxies on the BPT diagram, as well as sources identified as Type 1 AGN by the presence of broad emission lines (Oh et al. 2015). Each galaxy in the AGN-HOST sample was matched by stellar mass (to within ±5%) and GZ 'smooth' and 'disc' vote fractions, p_s and p_d (to within ±0.1) to at least one, and up to five, inactive galaxies to give 6107 galaxies. We refer to this sample as the INACTIVE sample. A Kolmogorov-Smirnov test revealed the redshift distributions of the INACTIVE and AGN-HOST samples are statistically indistinguishable ($D \sim 0.16$, $p \sim 0.88$).

Since this investigation is focussed on whether an AGN can have an impact on the SF of its host galaxy, we must consider whether there is a selection effect present in this identification method. The extent to which SF could be obscured by AGN emission was addressed by Schawinski et al. (2010). They showed, through a simple empirical experiment which simulated the addition of an AGN of known luminosity to a star forming galaxy, that BPT-based selection of AGN produces a complete sample, even in the blue cloud, at luminosities of $L[OIII] > 10^{40}$erg s^{-1}. Above this limit we therefore assume we have selected a complete sample of AGN independent of host galaxy SFR.

We also split both the AGN-HOST and INACTIVE samples into low, medium and high mass ranges (see Table 1) to investigate any trends in the SFH with mass. The mass boundaries were chosen to give roughly equal numbers of inactive galaxies in each bin prior to the mass matching to the AGN-HOST sample. Masses were calculated using the $(u-r)$ colour and absolute r-band magnitude with the method outlined in Baldry et al. (2006).

3 RESULTS

Figures 3 and 4 show the summed posterior probability distributions for the quenching time, t_q and exponential quenching rate, τ, respectively. In each figure the summed 1-dimensional normalised posterior probability distribution across the given parameter is shown for smooth and disc dominated galaxies across three mass bins for the AGN-HOST and INACTIVE samples. In Table 1 the percentage of the summed posterior distribution in each quenching regime for rapid ($\tau < 1$ Gyr), intermediate ($1 < \tau$ [Gyr] < 2) and slow ($\tau > 2$ Gyr) quenching timescales, are shown. Errors on the percentages are calculated from the range of values spanned by $N = 1000$ bootstrap iterations each sampling 90% of the population.

It is immediately apparent from Figures 3 and 4 that

Table 1. Table showing the number of galaxies in each of the three mass bins for both the AGN-HOSTS and INACTIVE galaxy samples and the percentage of the summed probability distribution across each morphologically weighted population found in the rapid, intermediate and slow quenching regimes.

SAMPLE	MASS BIN	WEIGHTING	$\tau < 1$ [Gyr]	$1 < \tau$ [Gyr] < 2	$\tau > 2$ [Gyr]	NUMBER
AGN-HOSTS	$\log[M_*/M_\odot] < 10.25$	p_d	$60\pm^{23}_{5}$	$13\pm^{9}_{9}$	$28\pm^{6}_{19}$	165(13.3%)
		p_s	$69\pm^{14}_{6}$	$17\pm^{6}_{14}$	$14\pm^{3}_{7}$	
	$10.25 < \log[M_*/M_\odot] < 10.75$	p_d	$33\pm^{3}_{5}$	$15\pm^{4}_{4}$	$51\pm^{4}_{7}$	630(50.6%)
		p_s	$69\pm^{4}_{5}$	$7\pm^{4}_{4}$	$26\pm^{5}_{9}$	
	$\log[M_*/M_\odot] > 10.75$	p_d	$20\pm^{5}_{4}$	$25\pm^{7}_{5}$	$56\pm^{8}_{12}$	449(36.1%)
		p_s	$24\pm^{4}_{3}$	$26\pm^{5}_{6}$	$50\pm^{7}_{7}$	
INACTIVE	$\log[M_*/M_\odot] < 10.25$	p_d	$37\pm^{8}_{14}$	$39\pm^{8}_{6}$	$24\pm^{6}_{6}$	807(13.2%)
		p_s	$47\pm^{5}_{11}$	$36\pm^{9}_{5}$	$17\pm^{4}_{5}$	
	$10.25 < \log[M_*/M_\odot] < 10.75$	p_d	$30\pm^{4}_{3}$	$18\pm^{2}_{3}$	$51\pm^{4}_{4}$	3094(50.7%)
		p_s	$42\pm^{2}_{2}$	$29\pm^{3}_{3}$	$30\pm^{3}_{4}$	
	$\log[M_*/M_\odot] > 10.75$	p_d	$36\pm^{3}_{3}$	$24\pm^{3}_{4}$	$41\pm^{4}_{3}$	2206(36.1%)
		p_s	$38\pm^{2}_{2}$	$28\pm^{3}_{4}$	$34\pm^{3}_{3}$	

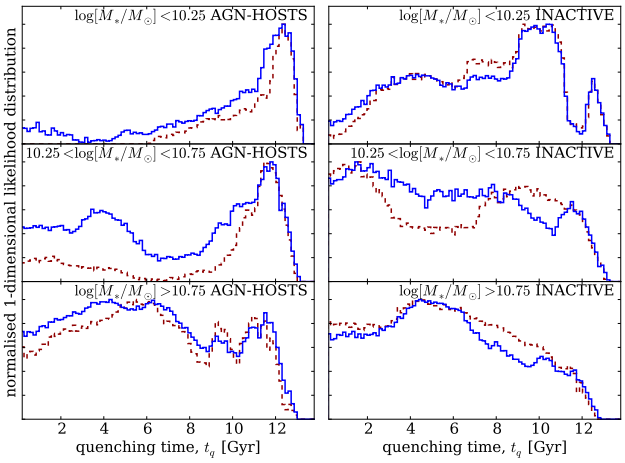

Figure 3. Normalised posterior probability distribution for the quenching time, t_q parameter normalised so that the areas under the curves are equal. AGN-HOST (left) and INACTIVE (right) galaxies are split into low (top), medium (middle) and high (bottom) mass for smooth (red dashed) and disc (blue solid) galaxies. A low value of t_q corresponds to the early Universe and a high value to the recent Universe.

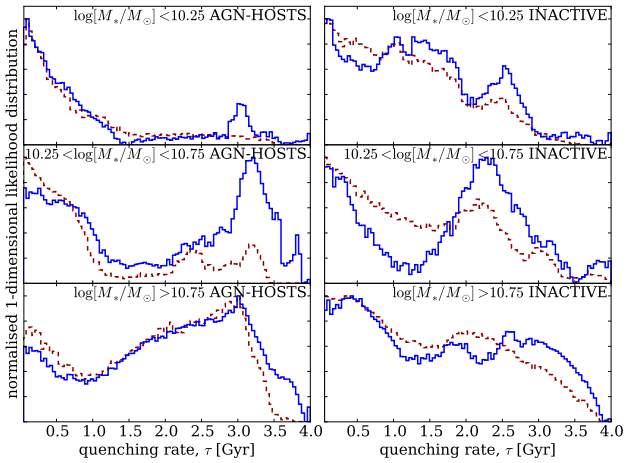

Figure 4. Likehood distribution for the quenching rate, τ normalised so that the areas under the curves are equal. AGN-HOST (left) host and INACTIVE (right) galaxies are split into low (top), medium (middle) and high (bottom) mass for smooth (red dashed) and disc (blue solid) galaxies. A small (large) value of τ corresponds to a rapid (slow) quench.

there is a distinct difference between the posterior probability distributions of AGN-HOST and INACTIVE populations.

At all masses, the posterior distribution for the AGN-HOST population across the quenching time t_q parameter (left panels of Figure 3) is different from that of the inactive galaxies (right panels of Figure 3). Recent quenching ($t >$ 11 Gyr) of AGN-HOST galaxies is the dominant history for low and medium mass galaxies, particularly for the smooth galaxy population. However, this effect is less dominant in higher mass galaxies where quenching at earlier times has significant probability.

The distributions of probability for the quenching rate, τ, in Figure 4 and Table 1 show the dominance of rapid quenching ($\tau < 1$ Gyr) across the AGN-HOST population, particularly for smooth galaxies. With increasing mass the dominant quenching rate becomes slow ($\tau > 2$ Gyr) especially for disc galaxies hosting an AGN. Similar trends in the probability are observed for the INACTIVE population but the overall distribution is very different.

The posterior probability distribution for the AGN-HOST galaxies therefore shows evidence for the dominance of rapid, recent quenching having occurred across the entire population. This result implies the importance of AGN feedback for the evolution of these galaxies.

4 DISCUSSION

The differences between the probability distribution of the AGN-HOST and INACTIVE galaxy populations reveal that an AGN can have a significant effect on the SFH of its host galaxy. Both recent, rapid quenching and early, slow quenching are observed in the probability distribution of the AGN-HOST population.

There are minimal differences between the smooth and disc weighted probability distributions of the quenching parameters across the AGN-HOST population. This is agreement with the conclusions of Kauffman et al. (2003b) who found

that the structural properties of AGN hosts depend very little on AGN power.

The difference between the AGN-HOST and INACTIVE population probability distributions in Figure 4 for the rate of quenching, τ, tells a story of gas reservoirs. The distribution of probability for higher mass AGN-HOST galaxies is dominated by slow, early quenching implying another mechanism is responsible for the cessation of star formation in these high mass galaxies prior to the triggering of the current AGN. This preference for slow evolution timescales follows from the ideas of previously isolated discs evolving slowly by the Kennicutt-Schmidt (Schmidt 1959; Kennicutt 1997) law which can then undergo an interaction or merger to reinvigorate star formation, feed the central black hole and trigger an AGN (Varela et al. 2004; Emsellem et al. 2015). These galaxies would need a large enough gas reservoir to fuel both SF throughout their lifetimes and the recent AGN. These high mass galaxies also play host to the most luminous AGN (mean $\log(L[OIII]$ [erg s^{-1}]) ~ 41.6) and so this SFH challenges the usual explanation for the co-evolution of luminous black holes and their host galaxies driven by merger growth.

Quenching at early times is also observed for the INACTIVE population, where the probability distribution for the quenching time is roughly constant until recent times where the distribution drops off. This drop-off occurs at earlier times with increasing mass with a significant lack of probability of quenching at early times for low mass INACTIVE galaxies (right panels Figure 3). This is evidence of downsizing across the entire INACTIVE galaxy population whereby stars in massive galaxies form first and quench early (Cowie et al. 1996; Thomas et al. 2010).

The most massive AGN-HOST galaxies also show a preference for earlier quenching (bottom left panel Figure 3) occurring at slow rates; we speculate that this is also due to the effects of downsizing rather than being caused by the current AGN. This earlier evolution would first form a slowly 'dying' or 'dead' galaxy typical of massive elliptical galaxies which can then have a recent infall of gas either through a minor merger, galaxy interaction or environmental change, triggering further star formation and feeding the central black hole, triggering an AGN (Kaviraj et al. 2014). In turn this AGN can then quench the recent boost in star formation. This track is similar to the evolution history proposed for blue ellipticals (Kaviraj et al. 2013; McIntosh et al. 2014; Haines et al. 2015). This SFH would then give rise to the probability distribution seen across the high mass AGN-HOST population for both time and rate parameters.

These recently triggered AGN in both massive disc and smooth galaxies do not have have the ability to impact the SF across the entirety of a high mass galaxy in a deep gravitational potential (Ishibashi et al. 2012; Zinn et al. 2013). This leads to the lower peak for recent, rapid quenching in the high mass AGN-HOST population for both morphologies.

Conversely, rapid quenching, possibly caused by the AGN itself through negative feedback, is the most dominant history for low mass AGN-HOST galaxies with lower gravitational potentials which allow gas to be expelled more easily (or heated by the AGN) across the entire galaxy (Tortora et al. 2009).

Tortora et al. (2009) model the effects of jet induced AGN feedback on a typical early type (i.e. smooth) galaxy and observe a drastic suppression of star formation on a timescale of $\sim$ 3 Myr. They convolve the SFR observed in their simulations with the models of Bruzual & Charlot (2003) to produce synthetic colours which are compared to the observed colours of a sample of SDSS elliptical galaxies, and find the time between the current galaxy age, t_{gal} and the time that the feedback began, t_{AGN}, peaks at $t_{gal} - t_{AGN} \sim 0.85$ Gyr. This agrees with the location of the peak in Figure 3 for low mass galaxies, where the difference between the peak of the probability and the average age of the population (galaxy age is calculated from the redshift by assuming all galaxies form at $t = 0$) is ~ 0.83 Gyr. This implies that this SFH dominated by recent quenching is caused directly by negative AGN feedback.

However, there still remains the possibility that the AGN is merely a consequence of an alternative quenching mechanism. This idea is supported by simulations showing that the exhaustion of gas by a merger fuelled starburst could cause such a rapid quench in star formation and in turn also trigger an AGN (Croton et al. 2006; Wild et al. 2009; Snyder et al. 2011; Hayward et al. 2014). Yesuf et al. (2014) also showed that AGN are more commonly hosted by post starburst galaxies, with the peak AGN activity appearing $\geqslant 200 \pm 100$ Myr after the starburst. Such a SFH is not accounted for in the models presented here, however this scenario is still consistent with the results presented in this paper; that AGN which are *currently* active have been detected in host galaxies ~ 1 Gyr after the onset of quenching.

This rapid quenching is particularly dominant for low-to-medium mass smooth galaxies. Smethurst et al. (2015) suggest that incredibly rapid quenching rates could be attributed to mergers of galaxies in conjunction with AGN feedback, which are thought to be responsible for creating the most massive smooth galaxies (Conselice et al. 2003; Springel, Di Matteo & Hernquist 2005; Hopkins et al. 2008). This dominance of rapid quenching across the smooth AGN-HOST population supports the idea that a merger, having caused a morphological transformation to a smooth galaxy, can also trigger an AGN, causing feedback and cessation of star formation (see Figure 14 of Schawinski et al. 2014).

For the medium mass AGN-HOST population we see a bimodal probability distribution between these two dominant quenching histories, highlighting the strength of this method which is capable of detecting such variation in the SFHs across a population of galaxies.

We have used morphological classifications from the Galaxy Zoo 2 project to determine the morphology-dependent star formation histories of a population of 1,244 Type 2 Seyfert AGN host galaxies, in comparison to an inactive galaxy population, via a Bayesian analysis of an exponentially declining star formation history model. We determined the most likely parameters for the quenching onset time, t_q, and exponential quenching rate, τ, and find clear differences in the combined population probabilities between inactive and AGN host galaxy populations. We have demonstrated a clear dependence on a galaxy currently hosting an AGN and its SFR. There is strong evidence for downsizing in massive inactive galaxies, which appears as a secondary effect in AGN host galaxies. The dominant quenching mechanism for galaxies currently hosting an AGN is for

rapid quenching which has occurred very recently. This result demonstrates the importance of AGN feedback across the entire host galaxy population, in driving the evolution of galaxies across the colour-magnitude diagram.

REFERENCES

Abazajian, K. N. et al., 2009, ApJS, 182, 543
Baldry, I. et al., 2006, MNRAS, 373, 469
Baldwin, J. A., Phillips, M. M., & Terlevich, R. 1981, PASP, 93, 5
Bamford, S. et al., 2009, MNRAS, 393, 1324
Blanton, M. R. et al., 2005, AJ, 129, 2562
Blanton, M. R. & Roweis, S., 2007, AJ, 133, 734
Bower, R. et al., 2006, MNRAS, 370, 645
Brinchmann, J. et al., 2004, MNRAS, 351, 1151
Bruzual, G. & Charlot, S., 2003, MNRAS, 344, 1000
Cardelli, J. A. et al., 1989, ApJ, 345, 245
Cisternas, M. et al., 2011, ApJ, 726, 57
Chabrier, G., 2003, PASP, 115, 763
Conselice, C. J. et al., 2003, AJ, 126, 1183
Cowie, L. et al., 1996, AJ, 112, 839
Cowie, L. & Barger, A. J., 2008, ApJ, 686, 72
Croton, D. J. et al., 2006, MNRAS, 365, 11
Emsellem, E. et al. 2015, MNRAS, 446, 2468
Fabian, A. C. 2006, ARA&A, 50, 455
Foreman-Mackey, D., Hogg, D. W., Lang, D., Goodman, J., 2013, PASP, 125, 306
Haines, T. et al., 2015, arXiv:1505.01493
Haring, N. & Rix, H-W., 2004, ApJ, 604, 89
Hayward, C. C. et al., MNRAS, 442, 1992
Hickox, R. C., et al., 2009, ApJ, 696, 891
Hopkins, F. et al., 2008, ApJSS, 175, 390
Ishibashi, W. et al., 2012, MNRAS, 427, 2998
Kauffman, G. et al., 2003, MNRAS, 341, 33
Kauffman, G. et al., 2003, MNRAS, 346, 1055
Kaviraj, S. et al., 2013, MNRAS, 428, 925
Kaviraj, S. et al., 2014, MNRAS, 440, 2944
Kennicutt, R. C., 1997, ApJ, 498, 491
Kewley, L. J. et al., 2001, ApJ, 556, 121
Kewley, L. J. et al., 2006, MNRAS, 372, 961
Kormendy, J. & Kennicutt, R. J., 2004, ARA&A, 42, 603
Lintott, C. J. et al., 2011, MNRAS, 410, 166
Magorrian, J. et al., 1998, AJ, 115, 2285
Marconi, A. & Hunt, L. K., 2003, ApJ, 589, 21
Martin, D. C. et al., 2005, ApJ, 619, L1
Martin, D. C. et al., 2007, ApJSS, 173, 342
McIntosh, D. et al., 2014, MNRAS, 442, 533
Noeske, K. G. et al., 2007, ApJ, 660, L47
Oh, K. et al., 2011, ApJS, 195, 13
Oh, K. et al. 2015, arXiv: 1504.07247
Padmanabhan, N. et al., 2008, ApJ, 674, 1217
Sarzi, M. et al., 2010, MNRAS, 402, 2187
Schawinski, K. et al., 2010, MNRAS, 711, 284
Schawinski, K. et al., 2014, MNRAS, 440, 889
Schmidt, M., 1959, ApJ, 129, 243
Silk, J. & Rees, M. J., 1998, A&A, 331, L1
Simmons, B. D. et al., 2011, ApJ, 734, 121
Singh, R. et al., 2013, A&A, 558, 43
Snyder, G. F. et al., 2011, ApJ, 741, 77
Smethurst, R. J. et al., 2015, MNRAS, 450, 435
Somerville, R. S. et al., 2008, MNRAS, 391, 481
Springel, V., Di Matteo, T. & Hernquist, L., 2005, ApJ, 620, L79
Taylor, M. B., 2005, ASP Conference Series, 347
Thomas, D. et al., 2010, MNRAS, 404, 1775
Tortora, C. et al., 2009, MNRAS, 369, 61
Varela, J. et al., 2004, A&A, 420, 873
Weiner, B. J. et al., 2006, ApJ, 653, 1049
Wild, V. et al., 2009, MNRAS, 395, 144
Willett, K. et al., 2013, MNRAS, 435, 2835
Yan, R. & Blanton, M. R. 2012, ApJ, 747, 61
Yesuf, H. M. et al., 2014, ApJ, 792, 84
York, D. G. et al., 2000, AJ, 120, 1579
Zinn, P. et al., 2013, ApJ, 774, 66

APPENDIX A: MASS MATCHED INACTIVE SAMPLE

Each galaxy in the AGN-HOST sample has been matched to at least one and up to five inactive galaxies. These were matched to within $\pm5\%$ of the stellar mass and ±0.1 of each of the disc and smooth GZ vote fractions, p_d and p_s.

Both the AGN-HOST and INACTIVE galaxy samples are shown on an optical-NUV colour colour diagram in Figure A1. The INACTIVE sample across all mass bins can be seen to encompass the entirety of the colour magnitude diagram, unlike the AGN-HOST sample which reside at increasingly green colours with increasing mass.

APPENDIX B: LUMINOSITY DEPENDENCE

An investigation into the dependence of the quenching in the AGN-HOST sample with $L[OIII]$ was also conducted, with the summed weighted posterior probability distributions for the quenching time and rate parameters shown in Figures B1 & B2. The AGN-HOST sample was split into low, medium and high luminosity as with the stellar mass. Since the $L[OIII]$ is dependent on the accretion rate, which is correlated with the mass of the black hole, which is in turn correlated with the stellar mass of the host galaxy, the stellar mass was used in the main investigation to allow a direct comparison to the control INACTIVE sample.

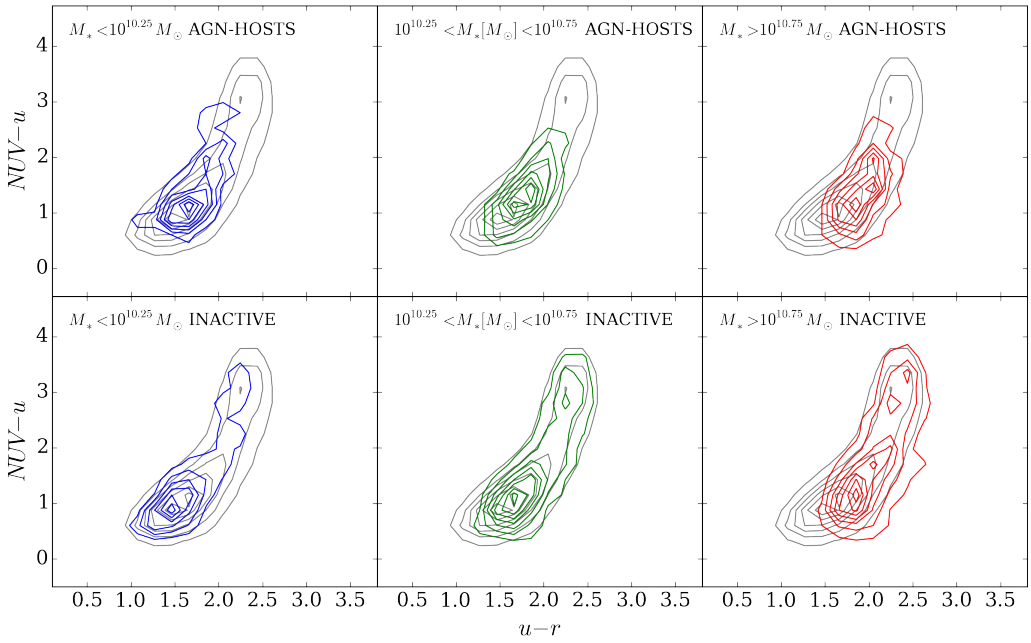

Figure A1. Optical-NUV colour-colour contour diagrams for the AGN-HOST (top) and INACTIVE galaxy samples split into low (blue), medium (green) and high (red) stellar mass samples. Underlaying each diagram are the contours of the GZ2-GALEX sample (grey).

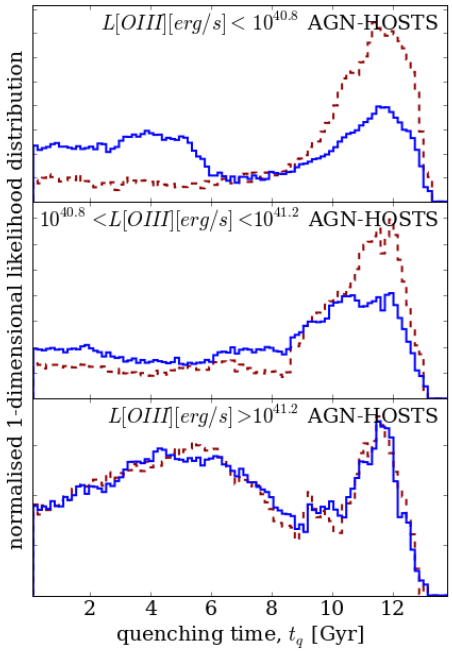

Figure B1. Likehood distribution for the quenching time, t_q normalised so that the areas under the curves are equal. AGN-HOST galaxies are split into low (top), medium (middle) and high (bottom) $L[OIII]$ for smooth (red dashed) and disc (blue solid) galaxies. A low value of t_q corresponds to the early Universe and a high value to the recent Universe.

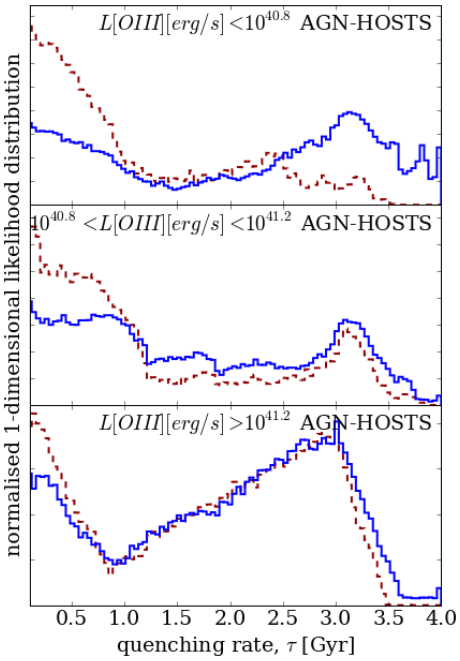

Figure B2. Likehood distribution for the quenching rate, τ normalised so that the areas under the curves are equal. AGN-HOST galaxies are split into low (top), medium (middle) and high (bottom) $L[OIII]$ for smooth (red dashed) and disc (blue solid) galaxies. A small (large) value of τ corresponds to a rapid (slow) quench.